Dewetting Dynamics of Nanofilled Polymer Thin Films

Haobin Luo and Dilip Gersappe*

Department of Materials Science and Engineering, State University of New York at Stony Brook, Stony Brook, New York 11794-2275

Received September 25, 2002; Revised Manuscript Received April 19, 2004

ABSTRACT: We use molecular dynamics simulations to study the dewetting dynamics of nanofilled polymer thin films on a substrate. We find that the addition of nanofillers can significantly retard the dewetting of polymer films. Our results show that to prevent dewetting the ideal situation is one in which the fillers are confined to the substrate/polymer interface, in agreement with previous experimental results. We find that the mechanism that controls the dewetting is not purely a result of a pinning effect but is also affected by the mobility of the filler particle, the interaction between the filler and the polymer, and the size of the nanofiller.

Introduction

Thin polymer films have been used extensively in a number of applications such as electronic packaging, lubricating surfaces, nonlinear optical devices, and lithography.[1,2] For such applications the formation of a homogeneous polymer layer on a solid substrate is necessary to achieve the desired properties. However, producing stable and defect-free thin polymer film is problematic since the polymer film tends to dewet the substrates. Studies have shown that as the polymer film gets thinner, its propensity to dewet increases.[3,4] As a result, there has been a great deal of interest in probing dewetting mechanisms and developing means by which the stability of thin polymer films on solid substrates can be improved.[5−22] These means range from using high molecular weight or glassy polymers to reduce the speed of dewetting, to modifying the substrate surface, by HF passivation,[17] by using grafted homopolymers[18] or random copolymers,[19] or simply by increasing the surface roughness.[20] Other alternatives include the modification of the polymer, such as the sulfonation and metal complexation of the polymer.[21] All these approaches, however, involve the chemical modification of the substrate and/or polymer and therefore have to be tailored for each particular system.

Recently, a novel approach to retard dewetting was proposed by Barnes et al.[22] in which they added C_{60} fullerene nanoparticles into the polymer before spin-casting the polymer film onto the substrate. With the addition of fullerenes they found that the dewetting of polymer films was greatly retarded or in some instances even totally prevented. They postulated that when the filler particles were confined to the substrate, the role of the filler particle was to act as an impurity and pin the contact line of the dewetting front. A retardation of dewetting was also reported when poly(benzyl ether) dendrimers were added to thin polystyrene films by Mackay et al.[23] In these experiments as well it was postulated that the surface segregation of the dendrimer, whose miscibility with polystyrene depends on its generation number, was an important factor in stabilizing the film. However, while these experiments clearly showed the potential of using nanofillers to prevent dewetting, since they concentrated on the use of fullerenes and dendrimers, they did not examine the role of other factors such as the size of the filler and the interaction between the filler and the polymer. To exploit the ability of filler particles to prevent the dewetting of polymer thin films, it is therefore necessary to understand the mechanism by which the fillers operate. Such knowledge will allow the rational design of filled polymer films that can resist dewetting.

In this paper, we use molecular dynamics (MD) simulations to determine the molecular mechanisms by which nanofillers can be used to prevent dewetting in polymer thin films. We find that, in order to prevent dewetting, the ideal situation is one when the fillers are confined to the substrate/polymer interface. We show that the mechanism that controls the dewetting is not purely a result of a pinning effect, but is also due to the local viscosity changes introduced by the addition of nanofillers. This effect is the largest when the fillers are immobile, but significant retardation is observed even when the fillers are mobile. Our simulations also show that the mobility of the filler particle, the interaction between the filler and the polymer, and the size of the nanofillers can all affect the ability of the filler to stabilize the film.

Model

Computer simulations have been extensively used in the study of fluid spreading, wetting, and drying phenomena on substrates.[24−30] The technique of choice in most of these simulations is molecular dynamics methods, and in this paper we also adopt a molecular dynamics to study the process of dewetting in filled polymer thin films.

The system that is modeled is a polymer thin film on top of an atomic substrate surface. The polymer is modeled as a linear chain with N segments. Monomers of mass m interact through a Lennard-Jones (L-J) potential of the form $V(r) = 4\epsilon[(\sigma/r)^{12} - (\sigma/r)^6]$ for $r < r^c = 2.2\sigma$. The potential is zero for $r > r^c$. Adjacent monomers along the chain are coupled by an additional FENE potential of the form $V_{CH}(r) = -0.5KR_0^2 \ln(1 - (r/R_0)^2)$ with $K = 30\epsilon$ and $R_0 = 1.5\sigma$.[31] Here σ and ϵ are the units of length and energy in the simulation, respectively. The substrate consists of atoms forming two (111) planes of an fcc lattice. The interaction between the polymer and the substrate is an L-J

* To whom correspondence should be addressed.

10.1021/ma025691t CCC: $27.50
Published on Web 07/02/2004

potential of the form of $V(r) = 4\epsilon[(\sigma/r)^{12} - \delta(\sigma/r)^6]$. The δ term is used to vary the wettability of substrate by the polymer. By varying the value of δ, we can modify the extent to which the polymer film "dislikes" the solid substrate, and a transition from wetting to partial dewetting to complete dewetting can be achieved.[27,30]

The nanofiller is modeled as a spherical particle interacting with the polymer and the wall with a modified L-J potential of the form of $V(r) = 4\epsilon_{ij}[(\sigma/(r - s))^{12} - (\sigma/(r - s))^6]$ for $r - s < r^c = 2.2\sigma$.[32] The filler−polymer interaction coupling is denoted as ϵ_{pf} and the filler−wall interaction coupling as ϵ_{wf}. Increasing values of ϵ_{pf} and ϵ_{wf} imply an increase in the attraction between the filler and the polymer and the filler and the wall, respectively. The filler size can be adjusted by modifying the parameter s. We focus mainly on nanofillers whose size is a little bigger than monomers by setting $s = 0.5$, which results in a filler radius, r_f, of 0.75σ. This is the filler size we use, if unspecified, in the simulation. The choice of this size of nanofiller was motivated by the experiments by Barnes et al. By using a filler radius of 0.75σ and a polymer chain length of 16, the size ratio between filler radius and radius of gyration (R_g) of the polymer chains is ~0.38. This is close to the value of about 0.4 we calculated from Barnes et al.'s work[22] by taking the radius of fullerene as 0.5 nm and the R_g of the polystyrene Barnes et al. used as 1.2 nm. Further, nanofillers of this size can easily be accommodated by the thin polymer films (e.g., the thickness of $\sim 5\sigma$ which we use) without introducing unwanted tensions. Nanofillers of different sizes (e.g., $r_f = 0.5\sigma$ or 1.25σ) are also used to probe the filler size effect in stabilizing polymer films.

The film is initialized with a lateral size of $80 \times 80\sigma$ and is made up of 1600 polymer chains of length 16. After equilibration the film thickness is $\sim 5\sigma$ or approximately 2.5 times the radius of gyration (R_g) of the unperturbed polymers. The temperature of the system is kept constant at $T = 1.1\epsilon/k_B$ (which is above the glass transition temperature of the polymer) by coupling the wall to a heat bath.[31] The density of the film is $0.81\sigma^{-3}$. Periodic boundary conditions are applied along the x and y directions to eliminate edge effects. The equations of motion are integrated using a fifth-order predictor−corrector algorithm with a time step of $\Delta t = 0.005\tau$, where $\tau = (m\sigma^2/\epsilon)^{1/2}$ and τ is the unit of time in the simulation. All our results are averaged over at least five independent starting configurations of the system.

In our simulation the dewetting condition is achieved by setting the value of δ to 0.75, which corresponds to a partial wetting condition.[27,30] The way we introduce dewetting is as follows. The polymer thin film is first fully equilibrated using a value of δ equal to 1.0. During the equilibration procedure, we track the radius of gyration of the chain, the motion of the center of mass of the chain, and the distribution of fillers inside the thin film to make sure that the system has completely equilibrated. After the equilibration step, to induce dewetting, we quench the system by instantaneously changing the value of δ to 0.75. In all the results presented below, the time reported is from the moment after the dewetting condition was applied.

Results and Discussion

Effect of Nanofillers on Dewetting Initiated by Thermal Fluctuations. For a nonwetting polymer film on top of a substrate, there are two types of mechanisms for the initialization of dewetting: spinodal decomposition and nucleation. If the polymer film is thick (e.g., thickness > 100 nm), dewetting occurs via the nucleation and growth of dry spots. If, on the other hand, the polymer film is thin, spinodal dewetting occurs via the amplification of thermal fluctuations in the thin film.[4] Although the mechanism of spinodal dewetting is well established in theoretical studies, direct experimental observation of the phenomena is quite limited.[5,6,10] This may due in part to the fact that both nucleation and spinodal decomposition can lead to dewetting of the unstable films. Nucleation occurs when contamination, such as dust and air bubbles in the film or on the surface, or an imperfection in the substrate exists. Under normal laboratory conditions, ideal systems for spinodal dewetting are hard to achieve. In the simulation, on the other hand, since we can eliminate all imperfections and defects on the surface, we can attempt to study the process of dewetting initiated by thermal fluctuations in the film. We note that while we cannot rule out the possibility of dewetting through homogeneous nucleation, studies on polymer films using parameters similar to ours have already established that spinodal dewetting is the primary destabilizing mechanism.[30]

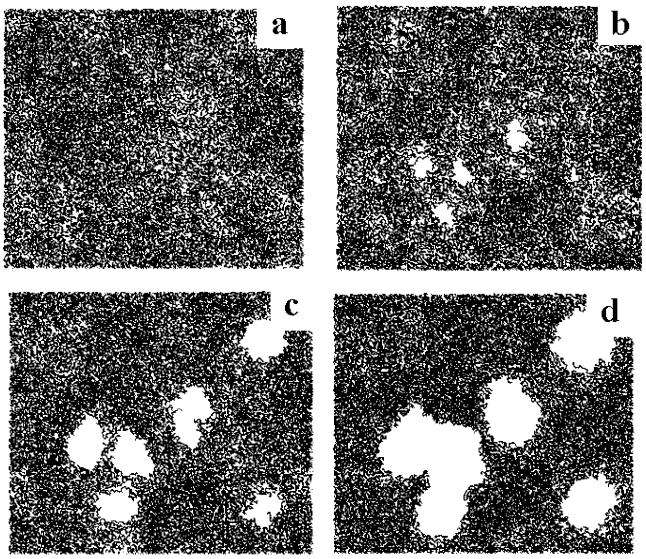

Figure 1. A time series of snapshots of the pure polymer thin film showing spinodal dewetting. The xy projection of the film is shown in these figures. (a) $t = 0\ \tau$; (b) $t = 75\ \tau$; (c) $t = 125\ \tau$; (d) $t = 175\ \tau$.

One of the first things we want to check is the effect of the nanofillers on the spontaneous dewetting behavior of polymer thin films. We start by observing the dewetting of both pure and filled polymer thin films. Shown in Figure 1 are representative snapshots for polymer thin films before and after dewetting occurs. For a pure polymer thin film before the dewetting condition is applied, no dewetting holes are formed and the film is homogeneous (Figure 1a). After the system is quenched to the point at which dewetting occurs, several holes begin to appear after time $t = 75\ \tau$ (Figure 1b). The holes continue to grow and merge into bigger ones when holes meet each other (Figure 1c,d). The growth of holes continues until the thin film is fractured. Since no impurity sites are present in our system and the substrate is both physically and chemically homogeneous, initiation of dewetting through nucleation is disfavored. This implies that the source of the observed

Table 1. Effect of Filler-wall Interaction (ϵ_{wf}) and Filler Volume Fraction on the Starting Time of Spinodal Dewetting

volume fraction by fillers (%)	starting time for dewetting (τ)				
	$\epsilon_{wf} = 1.0$	$\epsilon_{wf} = 3.0$	$\epsilon_{wf} = 6.0$	$\epsilon_{wf} = 10.0$	frozen fillers
8.0	40 ± 24	300 ± 185	725 ± 786	1000 ± 1112	1429 ± 1305
12.0	75 ± 35	1840 ± 1759	5905 ± 6826	no dewetting	no dewetting

dewetting behavior is a result of thermal instabilities. We test this by carrying out simulations on thicker films, and as expected we find that the initiation of dewetting is slowed and the hole density is decreased as the film gets thicker. Thus, our results are in agreement with what one would expect if thermal fluctuations are responsible for dewetting. The fast appearance and growth of dewetting holes for pure polymer films indicates the strong intrinsic instability of thin films on a nonwettable substrate. We then proceed to study the effect of introducing nanofillers in the film. The nanofillers we chose have a moderate attraction with the polymer, with ϵ_{pf} (the interaction between the polymer and the filler) set to be 2.0. (With a ϵ_{pf} value less than for example $\sim$1.6, the interaction between fillers and polymers is weak and the fillers form aggregates.) The filler distribution can be adjusted by varying the interaction strength between filler and substrate (ϵ_{wf}). We start by examining a filled system with 8.0 vol % of fillers distributed uniformly in the film. By setting the filler−wall interaction, $\epsilon_{wf} = 1.0$, we prevent the fillers from localizing near the wall surface. For this system, however, no retarding effect by nanofillers is observed as dewetting holes emerge soon after the filled films are quenched (Figure 2a) and the holes

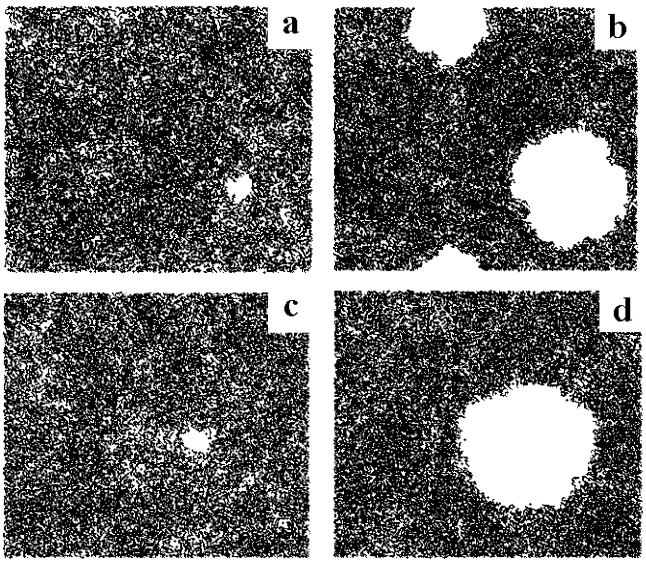

Figure 2. A time series of snapshots of the polymer thin film with an 8.0% volume fraction of nanofillers showing spinodal dewetting. The *xy* projection of the film is shown in the figure. For these runs, the parameters used are $\epsilon_{pf} = 2.0$ and $r_f = 0.75\sigma$. (a) $\epsilon_{wf} = 1.0$, $t = 100\ \tau$; (b) $\epsilon_{wf} = 1.0$, $t = 250\ \tau$; (c) $\epsilon_{wf} = 6.0$, $t = 1925\ \tau$; (d) $\epsilon_{wf} = 6.0$, $t = 2225\ \tau$.

grow at a similar rate, when compared to the unfilled polymer films (Figure 2b). When compared to the dewetting of the pure polymer film, the only noticeable difference is the decreased number density of dewetting holes. When the nanofillers are distributed in the polymer film (and not confined to the polymer/substrate interface), our simulations show that they can also have a detrimental effect on the dewetting. If the interaction between filler and polymer is too weak (e.g., $\epsilon_{pf} = 1.5$), nanofillers tend to aggregate, which introduces holes and no retarding effect can be achieved. If, on the other hand, the interaction between the filler and the polymer is too strong (e.g., $\epsilon_{pf} = 6.0$), we find that holes are formed during the equilibration procedure itself because for these thin films, the polymers prefer to coat the fillers rather than form a uniform film on the surface.

In contrast to the case when the fillers are distributed inside the polymer film, we find that there is a strong retarding effect when the fillers are localized at the substrate surface. By setting ϵ_{wf} to 6.0, the interaction between the nanofiller and the wall is much more favorable when compared to the interaction between the filler and the polymer. The fillers stay on the substrate surface and distribute evenly on the plane of the surface (Figure 3). As shown in Figure 2c,d dewetting still

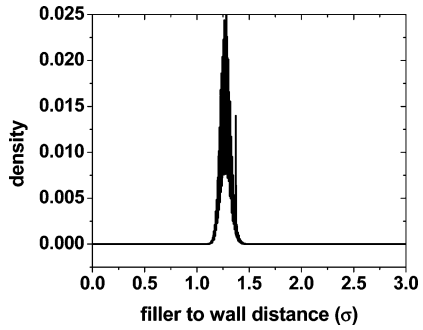

Figure 3. Filler density profile as a function of the distance from the substrate. For these runs we fix $\epsilon_{pf} = 2.0$, $\epsilon_{wf} = 6.0$, and $r_f = 0.75\sigma$. Note that the fillers distribute only on the substrate surface.

occurs, but at a much later time and with a much slower rate. Thus, these simulations recover the experimental observations of Barnes et al.,[22] where the localization of fillers at the substrate was thought to be key to the prevention of dewetting.

To further probe the effect of localizing the fillers at the substrate surface in Table 1, we list the time when dewetting first begins for filled systems with various filler−substrate interaction and different filler volume fractions. In all these runs we fix the value of $\epsilon_{pf} = 2.0$. Note that as we increase filler−substrate interaction, more and more fillers are attracted to the substrate surface until finally almost all the fillers distribute on the substrate surface (this happens at $\epsilon_{wf} = 6.0$). To determine the role of the filler in pinning the contact line, we also list in Table 2 the in-plane (*xy*) diffusion constants for both the polymer chains and the fillers for filled systems with filler volume fraction of 8.0% and 12.0%, respectively. For polymer films on top of a substrate, the chains that are close to the substrate should have a different diffusivity than the chains that are not in direct contact with the substrate. To better characterize the pinning effect played by fillers distribute on the substrate surface, in the calculation of the diffusion constant for the polymer chains, we categorize them into two groups: the inner layer group whose center of mass is within a radius of gyration (R_g) distance from the substrate surface and the upper layer

Table 2. Lateral Diffusion Constants for Polymers and Fillers in Filled Systems with a Filler Radius of 0.75σ

	pure polymer film	8.0 vol % filled films				12.0 vol % filled films			
		$\epsilon_{wf} = 3.0$	$\epsilon_{wf} = 6.0$	$\epsilon_{wf} = 10.0$	$\epsilon_{wf} = 6.0$ $\epsilon_{pf} = 4.0$	$\epsilon_{wf} = 3.0$	$\epsilon_{wf} = 6.0$	$\epsilon_{wf} = 10.0$
$4D_{\text{upper layer}}{}^{a}$ (σ^2/τ)	0.0520 ± 0.0013	0.0441 ± 0.0025	0.0446 ± 0.0009	0.0376 ± 0.0008	0.0253 ± 0.0009	0.0428 ± 0.0021	0.0430 ± 0.0016	0.0362 ± 0.0017
$4D_{\text{inner layer}}{}^{b}$ (σ^2/τ)	0.0403 ± 0.0032	0.0304 ± 0.0016	0.0308 ± 0.0013	0.0223 ± 0.0005	0.0108 ± 0.0009	0.0275 ± 0.0016	0.0293 ± 0.0017	0.0186 ± 0.0011
$4D_{\text{filler}}{}^{c}$ (σ^2/τ)	N/A	0.0426 ± 0.0018	0.0440 ± 0.0013	0.0189 ± 0.0007	0.0087 ± 0.0006	0.0413 ± 0.0009	0.0422 ± 0.0022	0.0145 ± 0.0004
Φ^{d} (%)	N/A	12.5	14.1	14.1	14.1	17.8	21.1	21.1

[a] $D_{\text{upper layer}}$ is the diffusion constant in the $x-y$ plane for polymer chains whose center of mass are at least at a distance of R_g from the substrate. [b] $D_{\text{inner layer}}$ is the diffusion constant in the $x-y$ plane for polymer chains whose center of mass are within a distance of R_g to the substrate. [c] D_{filler} is the diffusion constant in the $x-y$ plane for the fillers which are attracted on the substrates. [d] Φ: the surface coverage by nanofillers.

group whose center of mass is beyond the R_g range. As can be seen from Table 2, the polymer chains in the inner layer diffuse slower than those in the upper layers. The filler−substrate interaction has a clear effect on the diffusivity of nanofillers. At lower values of the filler−substrate interaction ($\epsilon_{wf} < 6.0$) the fillers move faster than the polymer chains. In other words, in this limit, the fillers cannot act as pinning sites. However, we still notice a reduction in the rate of dewetting which may be due to an increase in the local viscosity caused by the presence of nanofillers as the diffusion constant for polymer chains is decreased when compared to the unfilled film. As we increase the filler−substrate interaction ($\epsilon_{wf} = 10.0$) the fillers diffuse slower than the polymer chains. Thus, at these large values of ϵ_{wf}, the fillers can act as pinning sites, and the retardation effect becomes more pronounced. Indeed, from the table we can see that, in this limit, the diffusion for the chains in the inner layer is reduced substantially.

In Barnes et al.'s study about the suppression of dewetting by adding nanoparticles,[22] it was strongly inferred that the retarding effect was due mainly to the formation of an fullerene enrichment layer at the solid boundary that "pins" the contact line of the growing dewetted regions. Our simulations confirm the importance of the distribution of fillers on substrate in retarding dewetting, though we find that the retardation of dewetting can also be achieved by mobile fillers. However, our results indicate that in order to completely suppress the dewetting two conditions are necessary: First, the fillers need to diffuse slower than polymer chains, and second, there should be a critical concentration of fillers on the surface. In our system we find that these conditions correspond to a case when $\epsilon_{wf} = 10.0$, and we have 12.0 vol % of filler in the system (see Table 1).

Note that a very thin polymer film (with a thickness of about $2.5R_g$) was used in the above simulation. Such a thin film requires the stringent condition of slower filler diffusion to achieve a total suppression of dewetting initiated by thermal fluctuations. A thicker film should be more spinodally stable, and our preliminary results on thicker films (with a thickness of around $4R_g$) show that dewetting can be completely prevented even when fillers diffuse faster than polymer chains.

Effect of Nanofillers on Dewetting Initiated via Nucleation. To study the dewetting dynamics in detail, we want to control the starting time of dewetting, which is hard to achieve if dewetting is initiated by thermal fluctuations (as can be seen by the large fluctuations in the starting times in Table 1). To overcome this limitation, we design the next set of simulations in which we study a system with a prenucleated hole. We introduce a hole in the system by putting a purely repulsive cylindrical potential around the center of simulation cell (Figure 4). The system is fully equilibrated before the instant removal of this cylindrical potential when the dewetting condition is applied. The dewetting then proceeds through the growing of the central hole. The following studies are then done on systems that have a prenucleated hole in the center. We focus on systems where fillers distributed mostly or solely on substrate surface in order to understand the mechanism by which these localized fillers prevent or retard dewetting.

Before we proceed with the study of the growth of the prenucleated central hole, we first check the possible

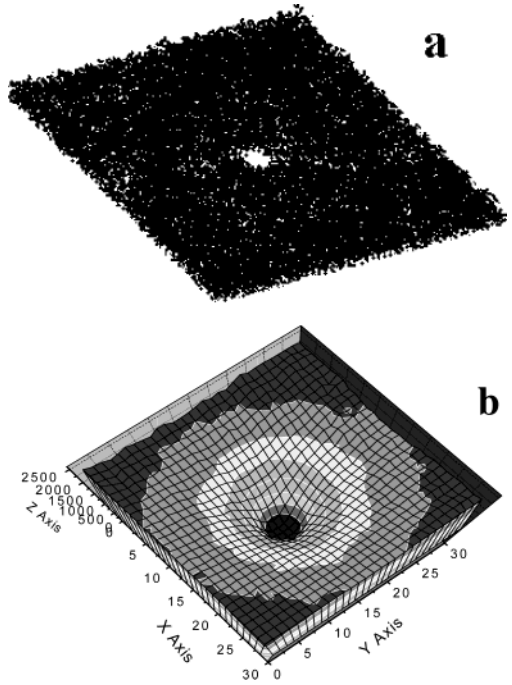

Figure 4. A prenucleated hole that is created by applying a purely repulsive cylindrical potential at the center of the simulation cell: (a) a snapshot; (b) accumulated density projection on the *xy* plane.

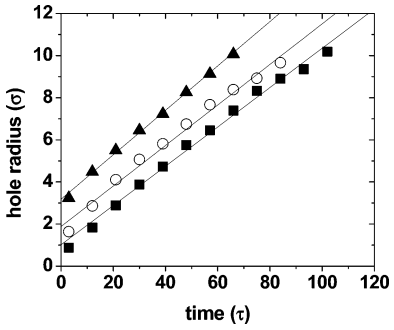

Figure 5. Dependence of the hole radius on time after dewetting is initiated for pure polymer thin films. Three different prenucleated hole radii are used. The lower curve corresponds to 0.9σ, the middle curve to 1.7σ, and the upper curve to 3.2σ. Note that in all three cases the rate of hole growth (given by the slope of the lines) is the same.

effect of different starting hole sizes on the dewetting dynamics. We find that the starting hole size does not affect the dewetting dynamics. Shown in Figure 5 is the dependence of the hole radius on time for pure polymer films with different starting hole radii. We can see that once the dewetting condition is applied, all the holes grow at the same rate independent of the size of the initial hole. The same observation also holds for the filled system with a filler radius of 0.75σ or less. This suggests that there is no residual tension around the equilibrated central hole and that our system size is large enough to prevent edge effects, as otherwise different growing rates are expected for different initiating hole sizes. We note that in the case of larger filler particles dewetting starts even before we quench the system to the dewetting condition, and therefore we cannot equilibrate a stable film with large filler particles.

By measuring the hole radius during dewetting, we can easily trace the effect of nanofillers on the dewetting dynamics. Shown in Figure 6 is the rate of hole growth

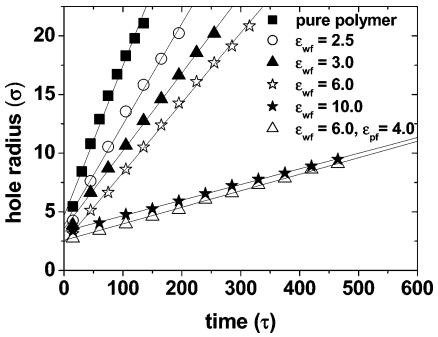

Figure 6. Dependence of hole radius on time for systems with a prenucleated central holes once dewetting is initiated The curve on top is for pure polymer system and the remaining ones are for the 8.0 vol % filled systems with mobile fillers of radius of 0.75σ. The slope for each curve (from top to bottom) is 0.1355 ± 0.0064, 0.0879 ± 0.0040, 0.0662 ± 0.0031, 0.0593 ± 0.0028, 0.0133 ± 0.0019, and 0.0137 ± 0.0025.

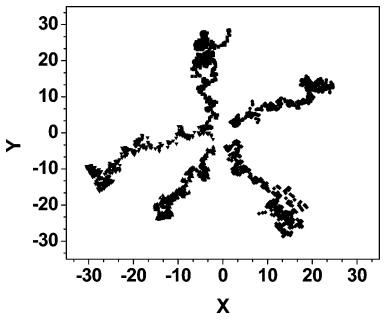

Figure 7. Traces of filler movements on the substrate surface during dewetting in 8.0 vol % filled films with $\epsilon_{pf} = 2.0$, $\epsilon_{wf} = 6.0$, and $r_f = 0.75\sigma$. Only fillers which are close to the hole front at the onset of hole growth are shown.

for various filler−wall interactions with an 8.0% volume fraction of nanofillers. Two effects should be noted from the figure: first, the hole grows linearly with time, and second, the nanofillers reduce the rate at which the hole grows. The stronger the filler−wall interaction, the more effective the retarding effect. For the mobile fillers, the retarding effect becomes especially pronounced when fillers move slower than polymer chains. There are two ways to make fillers move slower than polymers, as can be seen from Table 2. One is to increase the filler−wall interaction (the case with $\epsilon_{wf} = 10.0$ and $\epsilon_{pf} = 2.0$), and the other is to increase the filler−polymer interaction (the case with $\epsilon_{wf} = 6.0$ and $\epsilon_{pf} = 4.0$). Once fillers move slower than polymer chains, the pinning role played by fillers can effectively slow down the hole growth (Figure 6).

We can now start to check the pinning effect played by nanofillers. How will nanofillers react in response to the receding of the hole front during dewetting? In Figure 7, traces of filler movement are shown for those fillers which are close to the hole front when the hole first begins to grow. These fillers can be seen to move radially away from the dewetting center, along with the hole front. This is similar to Ohara and Gelbart's observation on the formation of annular rings made of nanometer-sized metal particles.[33] During the evaporation of volatile hexane solutions, the dissolved passivated metal particles were pushed radially along the liquid rim as the contact line receded. They observed the accumulation of particles along the rim. The contact line was finally pinned when there was sufficient number of accumulated particles. In our simulation, however, we do not find the enrichment of nanofillers

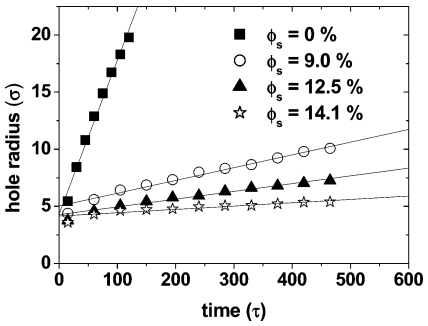

Figure 8. Dependence of hole radius on time for the 8.0 vol % filled systems with frozen fillers once dewetting is initiated. Here, $\epsilon_{pf} = 2.0$ and $r_f = 0.75\sigma$. The curve on top is the hole growth for the pure polymer system, which is shown here for comparison. In the figure, ϕ_s denotes the surface coverage by frozen fillers. The slope for the curves (from top to bottom) is 0.1355 ± 0.0064, 0.0112 ± 0.0020, 0.0068 ± 0.0019, and 0.0029 ± 0.0017.

along the receding front. Except for the tendency to be pushed away from the drying surface, the filler distribution does not have any pronounced changes.

Our results thus demonstrate that a retardation of dewetting can also be achieved when the fillers are mobile. To distinguish this mechanism from a pure "pinning" effect, we design the next series of simulations in which we "freeze" the filler particles. In the simulation, after equilibration is achieved, the position of the filler particles are frozen; i.e., no movement of the fillers is allowed. All other conditions are kept the same. The central hole growth dynamics in the presence of "frozen" fillers is shown in Figure 8. When compared to the situation where the fillers can move, the hole grows at a very suppressed rate. Indeed, as expected, the ideal situation is one when all the fillers are on the surface and are rendered immobile. However, even without this stringent condition dewetting can still be prevented by localization of the filler particles at the substrate surface.

Effect of a Patterned Surface on Dewetting. An additional factor that we have to consider is that we are changing the interaction between the polymer and the substrate when the fillers are confined to the substrate surface. For example, one could argue that the retardation of dewetting is simply a result of "patterning" the surface with patches that have a slight attraction to the polymer. In the next series of simulations, we test this possibility by using a patterned surface. To make the best match to conditions when the fillers are "frozen" to their positions, the patch positions are chosen according to the projection of "frozen" filler positions on the substrate. In this way different patterns, which correspond to their respective filler surface coverage, can be made. The patch−polymer interaction is set to be equal to the filler−polymer interaction. As a result, in these simulations, the size effect of fillers is excluded from the dewetting mechanisms.

Dewetting on these patterned surfaces is initiated by applying the dewetting condition only to those parts of the surfaces that are not the patches. As can be seen from Figure 9, in the presence of the substrate patches, the central hole grows faster than corresponding situations when there were "frozen" fillers on substrates. Besides the dewetting of preformed central hole, new drying sites also emerge and dewet, which was not observed in filled systems. Without the physical existence of nanofillers, the film is very unstable even though certain parts of the substrate (patches) are attractive to the polymer chains.

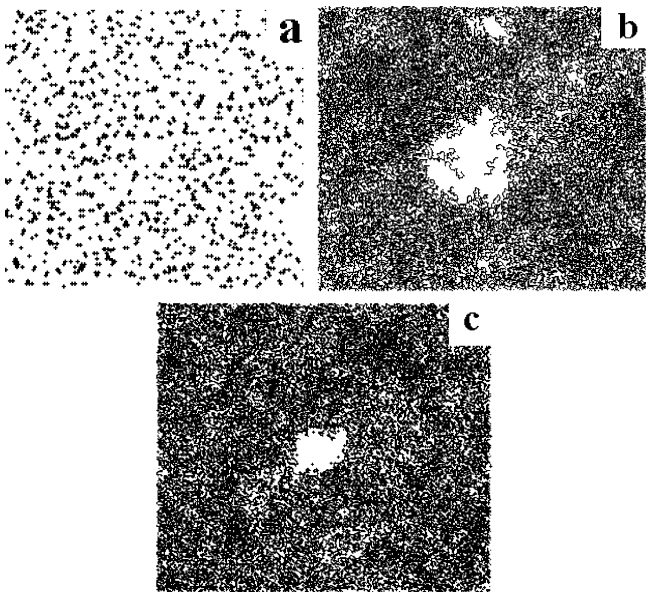

Figure 9. Dewetting on a patterned surface. (a) The *xy* projection of patches on the substrate that is used in the simulation. The patches correspond to a surface coverage of 14.1%. (b) The snapshot which shows the dewetting of the prenucleated central hole at $t = 500\tau$. The dewetting occurs on the patchy surface shown in (a). The patch−polymer interaction strength is set as $\epsilon = 2.0$. (c) The snapshot for the 8.0 vol % filled system with frozen fillers at the same time of $t = 500\tau$. The filler radius is 0.75σ, and the surface coverage by fillers is 14.1%. Note that the presence of fillers retards the dewetting when compared to the patterned surface.

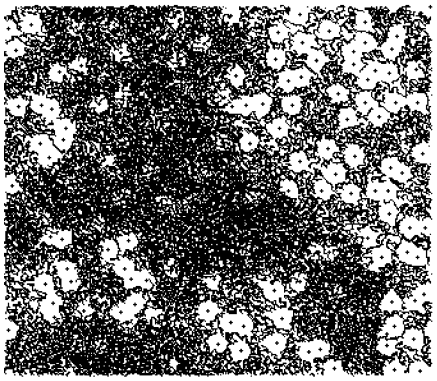

Figure 10. A MD snapshot for the 8.0 vol % filled system with a filler radius of 1.25σ. Holes introduced by the local tension around filler particles can be seen across the film.

Size Effect of Nanofillers. The simulation results shown so far are all done on fillers which have an effective radius of 0.75σ. Note this study is done on thin polymer films with a thickness of around 5σ. A problem with the simulation is that we cannot increase the filler size by a large amount (e.g., $r_f = 1.25\sigma$) as holes are formed around some fillers, even before dewetting is turned on (Figure 10). We believe this is a result of the large local tensions introduced by these large fillers. As a result, to determine the effect of filler size on dewetting behavior, we need to use either thicker films or smaller fillers. Since thicker films take a much longer time to equilibrate, we opt to use smaller filler sizes. The small fillers we choose have a radius of 0.5σ, which is of the same size as the bond length of the polymer. To compare the effect of smaller fillers vs larger fillers we use as our reference the 8.0 vol % filled systems with

Table 3. Lateral Diffusion Constants for Polymers and Fillers in Filled Systems with a Filler Radius of 0.5σ

	5.6 vol % filled films		8.0 vol % filled films	
	$\epsilon_{wf} = 6.0$	$\epsilon_{wf} = 10.0$	$\epsilon_{wf} = 6.0$	$\epsilon_{wf} = 10.0$
$4D_{\text{upper layer}}{}^{a}$ (σ^2/τ)	0.0399 ± 0.0024	0.0383 ± 0.0015	0.0364 ± 0.0008	0.0370 ± 0.0007
$4D_{\text{inner layer}}{}^{b}$ (σ^2/τ)	0.0293 ± 0.0009	0.0269 ± 0.0011	0.0242 ± 0.0011	0.0233 ± 0.0014
$4D_{\text{filler}}{}^{c}$ (σ^2/τ)	0.0752 ± 0.0023	0.0756 ± 0.0019	0.0672 ± 0.0011	0.0651 ± 0.0027
Φ^{d} (%)	14.1	14.1	20.0	20.0

[a] $D_{\text{upper layer}}$ is the diffusion constant in the $x-y$ plane for polymer chains whose center of mass are at least at a distance of R_g to the substrate. [b] $D_{\text{inner layer}}$ is the diffusion constant in the $x-y$ plane for polymer chains whose center of mass are within a distance of R_g to the substrate. [c] D_{filler} is the diffusion constant in the $x-y$ plane for the fillers which are attracted on the substrates. [d] Φ: the surface coverage by nanofillers.

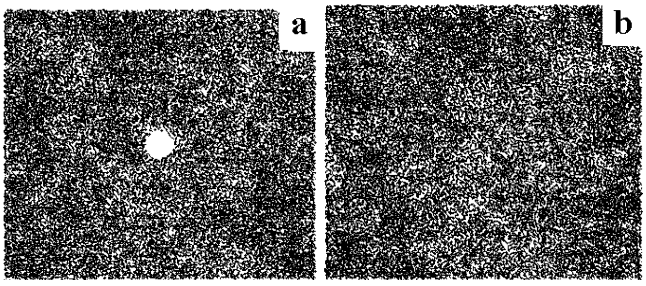

Figure 11. MD snapshots which show the "healing" of the prenucleated hole in the 8.0 vol % filled films with filler radius of 0.5σ. (a) At $t = 0\ \tau$, the initial hole radius is ~4.1σ. (b) At $t = 125\ \tau$, the prenucleated hole is already "healed".

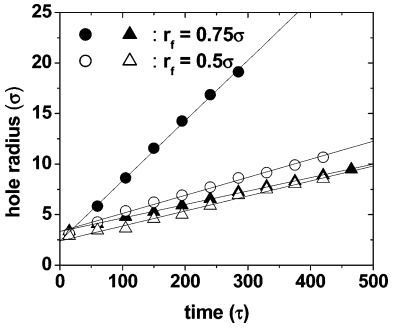

Figure 12. Effect of filler size on hole growth dynamics for filled systems with a filler surface coverage of 14.1%. The curves with filled symbols have a filler radius (r_f) of 0.75σ, while the open symbols correspond to systems with filler radius of 0.5σ. The curves with circular symbols (filled and open) have a $\epsilon_{wf} = 6.0$ while those with triangular symbols (filled and open) have a $\epsilon_{wf} = 10.0$. The slope for each curves (from top to bottom) is 0.0593 ± 0.0028, 0.0179 ± 0.0031, 0.0133 ± 0.0019, and 0.0148 ± 0.0012.

filler radius of 0.75σ. Note that for the reference systems when the larger fillers are all distributed on the substrate surface, the surface coverage is 14.1%.

For the first set of simulations we fix the volume fraction of fillers; i.e., we use systems which have the same filler volume fraction of 8.0%. We further restrict ourselves to the situations where fillers distribute only on the substrate by setting the filler−substrate interaction ϵ_{wf} to be 6.0 or 10.0. At a volume fraction of 8.0%, the surface coverage by these small fillers is 20.0%. Our simulations show that at these large surface coverage the retarding effect of the fillers is very strong, and the prenucleated central holes fail to grow. Instead, the holes are "healed" after the dewetting condition is turned on (Figure 11).

We then ran a series of simulations in which we fixed the surface coverage of the smaller fillers to be the same as that of the reference system. (To achieve the same amount of surface coverage as the larger fillers, we have to decrease the volume fraction of smaller fillers to 5.6%.) The hole growth dependence on time for both filler sizes is shown in Figure 12. From the figure we can see that the smaller fillers are very effective in retarding hole growth. In the smaller filler systems, with filler−substrate interaction set to $\epsilon_{wf} = 6.0$ or $\epsilon_{wf} = 10.0$, the hole growth rates are almost identical to that of larger fillers with strong filler−substrate interaction of $\epsilon_{wf} = 10.0$. However, while the retardation in the larger filler system with $\epsilon_{wf} = 10.0$ can be attributed to the pinning role of nanofillers as these larger fillers move slower than polymer chains (Table 2), the retardation that we see in the smaller filler system cannot be explained in the same way. We can see from Table 3 that the small fillers move much faster than polymer chains even in the systems where the filler−substrate interaction is as high as $\epsilon_{wf} = 10.0$. Despite the fast movement of the small filler particles, however, the diffusion of polymer chains close to the substrate surface is slowed to a rate which is comparable to that of larger filler systems when $\epsilon_{wf} = 10.0$. Therefore, we believe that the retardation in smaller filler systems is due to the enhancement of polymer viscosity, which results from the attractive polymer−filler interaction and is not a result of the pinning effect.

To further confirm that the pinning effect is not the operative mechanism for these very small mobile fillers, we designed the next series of simulations in which we fixed the number of pinning points at the surface to be the same as the larger fillers. We then proceeded to "freeze" these smaller fillers on the surface. We found that when compared to the reference systems with frozen fillers, not only do the prenucleated holes grow faster but also new holes emerge and grow. This implies that the smaller fillers cannot effectively "pin" the contact line and that the pinning effect increases as the size of the filler increases. In contrast, for mobile fillers, smaller fillers appear to be more effective at retarding dewetting.

Conclusion

The dewetting of polymer thin films on substrate can be retarded or totally prevented by the addition of nanosize fillers. The distribution of nanofillers on substrate is a key factor in this retarding effect as can be seen from the weak retardation shown when fillers distribute inside polymer films. Though the pinning effect by immobile nanofillers on the substrate surface is the most effective at retarding dewetting, mobile fillers can also achieve a total suppression of dewetting.

Our results indicate that there are two mechanisms that control the ability of the nanofiller to prevent dewetting of thin films. When the nanofiller is mobile, we believe that the retardation of dewetting is caused by an increase in the local viscosity of the polymer caused by the polymer−filler attraction.[34] When the nanofiller is immobile, the effect is similar to increasing

the surface roughness, i.e., a pinning effect. For mobile fillers, the key is the ability of the filler to increase the local viscosity of the polymer near the substrate. Smaller fillers are more effective at increasing the local viscosity, even when the surface area of the smaller filler particles is the same as that of the larger particles. We note that this behavior is analogous to the toughening mechanisms observed in polymer matrices reinforced with spherical nanofillers, where it was found that the greater mobility of the smaller filler particle was responsible for its superior properties.[35] We believe that the ability of the smaller, mobile fillers to act as temporary cross-linking sites, thus forming a network-like structure, could be key to its ability to enhance the local viscosity. On the other hand, if the fillers are "frozen", the key is the surface roughness, i.e., the size of the filler particle. Our simulations show that for "frozen" fillers, when the number of pinning sites are the same, large fillers are better at stabilizing the thin film. One important caveat in the use of larger filler particles, however, is that if the filler is too big (comparable to the film thickness), the large strains induced by the addition of larger filler particles can result in spontaneous dewetting.

Of the two effects, the local viscosity and the pinning effect, we find that the pinning effect is much better at preventing dewetting. We further find that when the filler is localized at the substrate surface, any factor that reduces the diffusion of the filler will increase the ability of the filler to retard dewetting. Our results can thus be used to design nanoparticles that can be used to increase the stability of thin films.

Acknowledgment. We thank Drs. Wentao Li and A. Karim for useful discussions. Funding from the NSF (DMR-0079410**)** is gratefully acknowledged.

References and Notes

(1) Cowie, J. M. G. *Polymers: Chemistry and Physics of Modern Materials*; Chapman and Hall: New York, 1991.
(2) Singh, J.; Agrawal, K. K. *J. Macromol. Sci., Rev. Macromol. Chem. Phys.* **1992**, *32*, 521−534.
(3) de Gennes, P. G. *Rev. Mod. Phys.* **1985**, *57*, 827−863.
(4) Brochard-Wyart, F.; Daillant, J. *Can. J. Phys.* **1990**, *68*, 1084−1088.
(5) Reiter, G. *Phys. Rev. Lett.* **1992**, *68*, 75−78.
(6) Reiter, G. *Langmuir* **1993**, *9*, 1344−1351.
(7) Brochard-Wyart, F.; de Gennes, P. G.; Hervert, H.; Redon, C. *Langmuir* **1994**, *10*, 1566−1572.
(8) Kerle, T.; Yerushalmi-Rozen, R.; Klein, J.; Fetters, L. J. *Europhys. Lett.* **1998**, *44*, 484−490.
(9) Kargupta, K.; Sharma, A. *Langmuir* **2002**, *18*, 1893−1903.
(10) Xie, R.; Karim, A.; Douglas, J. F.; Han, C. C.; Weiss, R. A. *Phys. Rev. Lett.* **1998**, *81*, 1251−1254.
(11) Stange, T. G.; Evans, D. F.; Hendrickson, W. A. *Langmuir* **1997**, *13*, 4459−4465.
(12) Karapanagiotis, I.; Evans, D. F.; Gerberich, W. W. *Langmuir* **2001**, *17*, 3266−3272.
(13) Seemann, R.; Herminghaus, S.; Jacobs, K. *Phys. Rev. Lett.* **2001**, *86*, 5534−5537.
(14) Masson, J. L.; Green, P. F. *Phys. Rev. E* **2002**, *65*, 031806.
(15) Renger, C.; Muller-Buschbaum, P.; Stamm, M.; Hinrichsen, G. *Macromolecules* **2000**, *33*, 8388−8398.
(16) van der Wielen, M. W. J.; Baars, E. P. I.; Giesbers, M.; Cohen Stuart, M. A.; Fleer, G. J. *Langmuir* **2000**, *16*, 10137−10143.
(17) Sung, L.; Karim, A.; Douglas, J. F.; Han, C. C. *Phys. Rev. Lett.* **1996**, *76*, 4368−4371.
(18) Henn, G.; Bucknall, D. G.; Stamm, M.; Vanhoorne, P.; Jerome, R. *Macromolecules* **1996**, *29*, 4305−4313.
(19) Mansky, P.; Russell, T. P.; Hawker, C. J.; Mays, J.; Cook, D. C.; Satija, S. K. *Phys. Rev. Lett.* **1997**, *79*, 237−240.
(20) Tolan, M.; Vacca, G.; Wang, J.; Sinha, S. K.; Li, C.; Rafailovich, M. H.; Sokolov, J.; Gibaud, A.; Lorenz, H.; Kotthaus, J. P. *Phys. B* **1996**, *221*, 53−59.
(21) Feng, Y.; Karim, A.; Weiss, R. A.; Douglas, J. F.; Han, C. C. *Macromolecules* **1998**, *31*, 484−493.
(22) Barnes, K. A.; Karim, A.; Douglas, J. F.; Nakatani, A. I.; Grull, H.; Amis, E. J. *Macromolecules* **2000**, *33*, 4177−4185.
(23) Mackay, M. E.; Hong, Y.; Jeong, M.; Hong, S.; Russell, T. P.; Hawker, C. J.; Vestberg, R.; Douglas, J. F. *Langmuir* **2002**, *18*, 1877−1882.
(24) Sikkenk, J. H.; Indekeu, J. O.; van Leeuwen, J. M. J.; Vossnack, E. O. *Phys. Rev. Lett.* **1987**, *59*, 98−101.
(25) Velasco, E.; Tarazona, P. *J. Chem. Phys.* **1989**, *91*, 7916−7924.
(26) Bresme, F.; Quirke, N. *Phys. Rev. Lett.* **1998**, *80*, 3791−3794.
(27) Voue, M.; de Coninck, J. *Acta Mater.* **2000**, *48*, 4405−4417.
(28) Milchev, A.; Binder, K. *J. Chem. Phys.* **1997**, *106*, 1978−1989.
(29) Liu, H.; Bhattacharya, A.; Chakrabarti, A. *J. Chem. Phys.* **1998**, *109*, 8607−8611.
(30) Koplik, J.; Banavar, J. R. *Phys. Rev. Lett.* **2000**, *84*, 4401−4404.
(31) Grest, G. S.; Kremer, K. *Phys. Rev. A* **1986**, *33*, 3628−3631.
(32) Nuevo, M. J.; Morales, J. J.; Heyes, D. M. *Phys. Rev. E* **1998**, *58*, 5845−5854.
(33) Ohara, P. C.; Gelbart, W. M. *Langmuir* **1998**, *14*, 3418−3424.
(34) Jaber, E.; Luo, H.; Li, W.; Gersappe, D. Manuscript in preparation.
(35) Gersappe, D. *Phys. Rev. Lett.* **2002**, *89*, 058301-1−058301-4.

MA025691T